galaxies

MDPI

Article

18–22 cm VLBA Observational Evidence for Toroidal B-Field Components in Six AGN Jets

Juliana Cristina Motter [1,2,*] and Denise Carmen Gabuzda [2]

1 Instituto de Astronomia, Geofísica e Ciências Atmosféricas, Universidade de São Paulo, São Paulo 05508-090, Brasil
2 Physics Department, University College Cork, Cork, Ireland; d.gabuzda@ucc.ie
* Correspondence: juliana.motter@usp.br; Tel.: +55-11-3091-2734

Academic Editors: Jose L. Gómez, Alan P. Marscher and Svetlana G. Jorstad
Received: 5 July 2016; Accepted: 26 August 2016; Published: 30 August 2016

Abstract: The formation of relativistic jets in Active Galactic Nuclei (AGN) is related to accretion onto their central supermassive black holes, and magnetic (**B**) fields are believed to play a central role in launching, collimating, and accelerating the jet streams from very compact regions out to kiloparsec scales. We present results of Faraday rotation studies based on Very Long Baseline Array (VLBA) data obtained at 18–22 cm for six well known AGN (OJ 287, 3C 279, PKS 1510-089, 3C 345, BL Lac, and 3C 454.3), which probe projected distances out to tens of parsecs from the observed cores. We have identified statistically significant, monotonic, transverse Faraday rotation gradients across the jets of all but one of these sources, indicating the presence of toroidal **B** fields, which may be one component of helical **B** fields associated with these AGN jets.

Keywords: AGN; relativistic jets; polarization; radio interferometry

1. Introduction

The synchrotron radiation detected from the relativistic jets of Active Galactic Nuclei (AGN) is intrinsically linearly polarized up to 75%, and indicates the presence of relativistic electrons accelerated by local magnetic (**B**) fields. Therefore, linear polarization studies provide information about the degree of order and the direction of the **B**-field in the emission region, and multiwavelength observations provide information about Faraday rotation occurring between the source and observer.

Faraday rotation occurs when a linearly polarized electromagnetic wave travels through magnetized plasma; the resulting difference in the speeds of the right and left-circularly polarized components of the wave causes the plane of polarization to rotate. The amount of rotation is given by

$$\chi_{obs} = \chi_o + RM\lambda^2, \quad \text{where} \quad RM \propto \int n_e \mathbf{B} \cdot d\mathbf{l} \tag{1}$$

where χ_{obs} is the observed polarization angle, χ_o is the unrotated polarization angle, λ is the observing wavelength, n_e is the electron density, and $\mathbf{B} \cdot d\mathbf{l}$ is the magnetic field times a path element along the line-of-sight. RM is the rotation measure, which can be determined by measuring the polarization angles at different wavelengths.

It was pointed out by Blandford [1] that, in the presence of a helical **B**-field, transverse Faraday rotation measure gradients should be observed across AGN jets, due to the systematic change in the line-of-sight component of the **B**-field. The detection of these gradients was first reported by Asada et al. [2], and more recently in the studies [3–8], providing evidence for the presence of an azimuthal (toroidal) field component which may be associated with helical fields threading these jets.

In this work, we present the results of Very Long Baseline Array (VLBA) Faraday rotation studies at 18–22 cm for six well-known AGN: OJ 287, 3C 279, PKS 1510-089, 3C 345, BL Lac, and 3C 454.3.

These six sources have been studied in a variety of contexts, including precessional models, jet motions in parsec scales, and multiwave-band variability [9–13]. These 18–22 cm observations are ideally suited for probing distances out to tens of parsecs from the observed core, and provide a link between the miliarcsecond (parsec) scale structures seen by the VLBA and the arcsecond (kiloparsec) scales seen by the VLA. Therefore, these six sources were chosen to provide results on scales not yet probed, so that structural and polarization variations on these different scales could be better understood.

2. Observations and Data Analysis

The observations analysed in this work were made simultaneously at 1358, 1430, 1493, and 1665 MHz (22.1, 21.0, 20.1, and 18.0 cm) with the National Radio Astronomy Observatory (NRAO) VLBA at various epochs in 2010 at a total aggregate bit rate of 128 Mbits/s, observing each source in snapshot mode [14]. The amplitude, phase, polarization, and electric vector position angle (EVPA) calibrations were done in the NRAO Astronomical Imaging Processing System (AIPS) using standard techniques, using Los Alamos as the reference antenna. VLA and (VLBI) observations of the compact polarized source J0006-0623 obtained at nearly simultaneous epochs were used for the EVPA calibrations, by rotating the EVPAs for the total VLBI polarization to agree with those for the VLA polarization.

Maps of the total intensity I and the Stokes parameters Q and U were done in AIPS using standard procedures, and the Q and U maps were used to make maps of the polarized flux, $p = \sqrt{Q^2 + U^2}$, and polarization angle, $\chi = \frac{1}{2}\tan^{-1}(\frac{U}{Q})$. The polarization angle maps used to make the RM maps were all convolved with the lowest-frequency beam to match their resolutions. We removed the effect of integrated Galactic foreground RM [15,16] before constructing the Faraday RM maps, and applied the results of [3] when estimating the RM uncertainties.

3. Results

We show in Figures 1 and 2, as examples, the RM maps of 3C 454.3 and 3C 279 superimposed on the 1358 MHz total intensity contours along with slices taken in regions where transverse RM gradients were detected. The ranges of the RM values are indicated by the color bars. The gray ellipse in the lower-left corner of each map depicts the convolving beam.

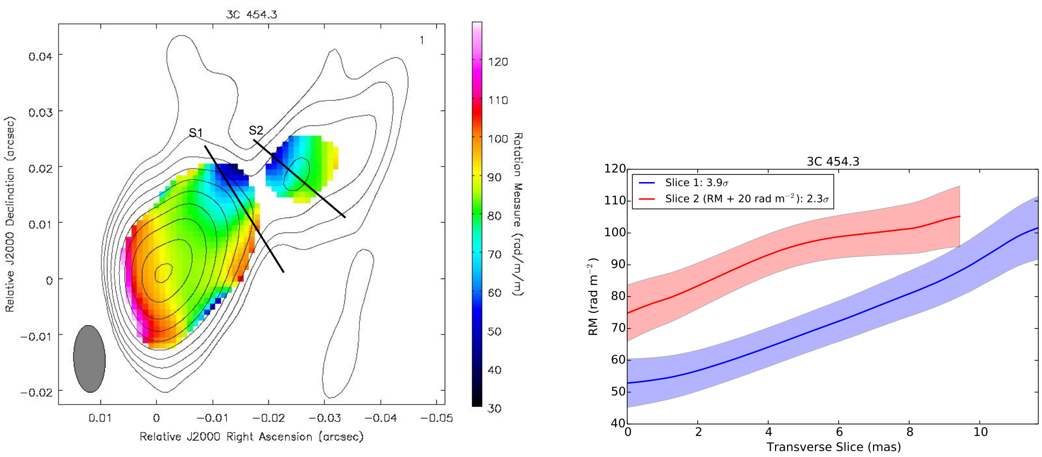

(**a**) (**b**)

Figure 1. (**a**) Rotation measure (RM) distribution for 3C 454.3 superimposed on the 1358 MHz *I* map. The bottom *I* contour is 0.25% of the peak of 4.06 Jy/beam, and the contours increase in steps of a factor of two. The black lines across the RM map show the locations of slices taken in regions where transverse RM gradients are visible, and the letter "S" indicates the side corresponding to their starting points. Output pixels were blanked for RM uncertainties exceeding 10 rad/m^2; (**b**) Transverse slices taken across the jet of 3C 454.3, with statistical significances of 3.9σ (Slice 1) and 2.3σ (Slice 2).

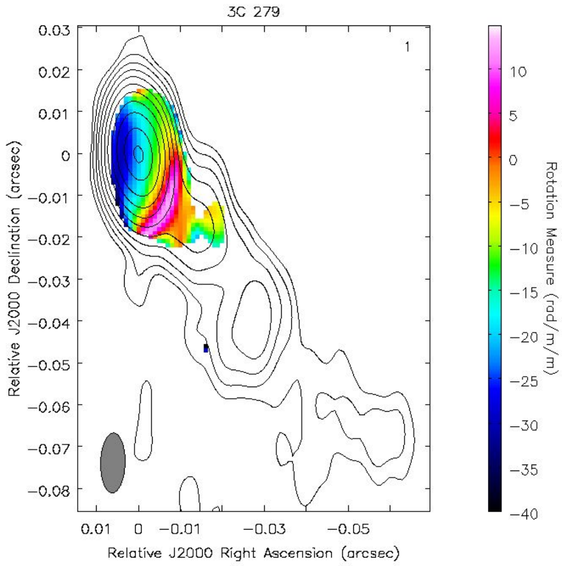

Figure 2. RM distribution for 3C 279 superimposed on the 1358 MHz *I* map. The bottom *I* contour is 0.125% of the peak of 3.47 Jy/beam, and the contours increase in steps of a factor of two. Output pixels were blanked for RM uncertainties exceeding 10 rad/m^2. Although an apparent RM gradient can be seen in the core, this gradient proved not to be robust and statistically significant.

We list in Table 1, for each of the transverse RM gradients detected in the six sources studied here, its location, width in beamwidths in the direction of the gradient, direction on the sky (clockwise or counter-clockwise relative to the base of the jet), and statistical significance. Four sources show transverse Faraday rotation gradients with statistical significances higher than 3σ, and the gradient across the jet of 3C 345 has a significance of 2.4σ. We detected sign changes in the RM values across the transverse gradients in the jets of OJ 287, PKS 1510-089, 3C 345, and BL Lac. All the gradients remain visible when the RM maps are produced using circular beams with areas roughly equal to the intrinsic elliptical beams.

Table 1. List of detected transverse RM gradients.

Source Name	Gradient Location	Gradient Width (Beamwidths)	Gradient [a] Direction	Statistical Significance
OJ 287	Core	1.4	CCW	4.4σ
PKS 1510-089	Core	2.4	CCW	4.4σ
3C 345	Jet	2.2	CW	2.4σ
BL Lac	Core	1.4	CCW	3.7σ
3C 454.3 (S1)	Jet	1.1	CW	3.9σ
3C 454.3 (S2)	Jet	1.4	CW	2.3σ

[a] CW denotes clockwise and CCW denotes counter-clockwise direction relative to the base of the jet (located upstream from the observed core).

4. Discussion

4.1. Reliability of the Detected Transverse RM Gradients in AGN Jets

Concern has been expressed in the literature about the reliability of the detection of transverse RM gradients across AGN jets, regarding the width of these gradients compared to the beam sizes of the observations. However, Monte Carlo simulations carried out by Mahmud et al. [4] and Murphy and Gabuzda [17] for VLBA data with realistic noise and baseline coverage and RM gradients having various widths and strengths convolved with beams of various sizes have shown that transverse RM gradients can still be visible, even if the intrinsic jet width is of the order of 1/20 of a beamwidth. The simulations of [17] have also shown that the spurious 3σ gradients arose in far less than 1% of the cases in simulations based on the same four wavelengths used in our study, even for jets much narrower than the beam sizes. This was also found to be true for 2σ gradients spanning at least two beamwidths. Considering these results, the transverse RM gradients listed in Table 1 can all be considered firm detections, including the one observed in 3C 345.

The detection of transverse RM gradients across AGN jets can be used as a diagnostic for the geometry of the magnetic field in these regions, since this provides evidence for the presence of a toroidal **B**-field component, which may be one component of helical **B**-fields associated with these jets. The detection of sign changes in the RM values across the jets of OJ 287, PKS 1510-089, 3C 345, and BL Lac favours this interpretation, since gradients in electron density could not cause this effect. Note, however, that the non-detection of a sign change across the jet of 3C 454.3 does not exclude the possibility that the transverse RM gradients are due to a toroidal **B**-field component, since some combinations of helical pitch angles and viewing angles give rise to gradients of a single sign.

4.2. Direction of the Transverse RM Gradients

The direction of the azimuthal (toroidal) component of a helical **B**-field threading an AGN jet should be determined by the direction of rotation of the central supermassive black hole and the accretion disc, along with the direction of the initial poloidal field that is wound up (inward or outward along the jet). One could intuitively think that these should both be random, and as a consequence, the direction of the RM gradients on the sky, relative to the direction of the jet, should also be random. One way to describe the direction of the RM gradients on the sky is to refer to them as being oriented clockwise (CW) or counter-clockwise (CCW) relative to the jet direction. In other words, if we think of the base of the jet (located upstream of the observed VLBI core) as the center of a clock, the direction of the RM gradient points in the CW or CCW direction (Figure 3).

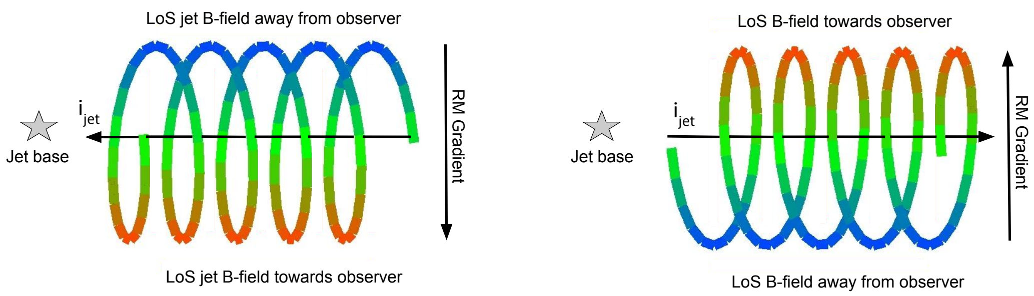

(**a**) (**b**)

Figure 3. In both panels, $\mathbf{i_{jet}}$ denotes the current in the jet, and the horizontal black arrow shows its direction along the jet. *LoS* denotes line-of-sight. The vertical black arrow on the right-hand side of each panel shows the direction of increase of the RM values. (**a**) A CW gradient as seen on the sky, which implies an inward jet current; (**b**) A CCW gradient as seen on the sky, which implies an outward jet current.

However, this intuitive idea that the direction of rotation of the black hole/accretion disc and the direction of the initial poloidal **B**-field are both random may not be correct. For example, the presence of an azimuthal (toroidal) **B**-field component implies the presence of an axial current in the jet; it is easy to imagine that the direction of this current—inward or outward along the jet—might not be random, due to various physical processes related to the launching and accelerating of the jet, as well as the composition of the jet itself (i.e., is it comprised primarily of equal-mass particles such as electrons and positrons, or of particles with very unequal masses, such as electrons and protons). If there is a preferential direction for the currents in the jets, this will lead to a preferential direction for the azimuthal **B**-field component, which will, in turn, lead to a preferential direction for the associated transverse RM gradients on the sky—CW (inward jet current) or CCW (outward jet current). The relationship between the direction of the azimuthal component of the helical jet **B**-field, the direction of the associated transverse RM gradient, and the direction of the implied jet current are shown in Figure 3.

Contopoulos et al. [18] claimed to have detected a preference of CW over CCW transverse RM gradients on parsec scales, based on RM maps previously published in the literature. However, their analysis was subject to uncertainty due to the inability at that time to derive accurate estimates of the statistical significances of these transverse RM gradients. A number of recent studies have been aimed at reanalyzing the previously published RM maps considered in [18] using the approach developed in [3] to more accurately and reliably estimate the uncertainties in the measured RM values and the statistical significances of detected transverse RM gradients [6,7]. The recent analysis of Christodoulou et al. [19], based on available RM maps on relatively large scales exceeding about 20 pc, has provided strong evidence for a preference for CCW RM gradients (or outward jet currents) on these larger scales. They suggest that the claim of [18] for a preference of CW RM gradients (inward jet currents) on parsec scales and their finding of a preference of CCW RM gradients (outward jet currents) on larger scales can be understood in terms of a single self-consistent system of fields and currents, with an inward current along the jet axis surrounded by inner and outer regions of helical field with opposite directions for their azimuthal components, with these two regions separated by a current sheet carrying outward current.

The scales probed by our observations fall near the transition between the scales considered in [18] and in [19], making it of interest to see whether our results provide any evidence for a preferred direction for the observed transverse RM gradients on these scales. The fourth column in Table 1 lists the directions on the sky of the detected transverse RM gradients. Three of them are CW on the sky relative to their jet bases, implying inward currents along their jets, and three are CCW, implying outward jet currents. Thus, there is no evidence in our results for the small number of sources we have considered for a preferential direction for the observed transverse RM gradients, and consequently for the currents flowing along the jets. This may be consistent with the model proposed by [19], but 18–22 cm RM maps for more AGN are required before any firm conclusions can be drawn.

5. Conclusions

We have presented results of Faraday rotation studies for six AGN through the analysis of VLBA data obtained at four wavelengths in the range 18–22 cm. We have identified monotonic, statistically significant, transverse Faraday rotation gradients across the jets of five of these sources: OJ 287, PKS 1510-089, 3C 345, BL Lac, and 3C 454.3. Smoothly varying, monotonic, transverse RM gradients indicate the presence of a toroidal **B** field component, which may be associated with helical **B** fields threading these AGN jets.

There is no evidence for a preferred direction for the transverse RM gradients on the sky (i.e., for a preferred direction of the predominant jet currents) on the scales probed by these observations. We highlight the importance of carrying out more studies in this wavelength range, considering the intermediate scales it probes, to provide a connection with what is seen in both parsec and kilo-parsec scales, and also to provide new observational evidence to be confronted with theoretical models of jet formation in AGN.

Acknowledgments: Juliana Cristina Motter thanks CAPES (Coordenação de Aperfeiçoamento de Pessoal de Nível Superior) for the financial support under the grant BEX 3421-15-5. We thank Sebastian Knuettel for sharing his expertise during the course of this research. This work has made use of data from the NRAO VLBA facilities.

Author Contributions: All the imaging and data analysis were made by Juliana Cristina Motter. Supervision, revision and suggestions were made by Denise Carmen Gabuzda.

Conflicts of Interest: The authors declare no conflict of interest.

References

1. Blandford, R.D. Acceleration and collimation mechanisms in jets. *Astrophys. Space Sci. Libr.* **1993**, *103*, 15–33.
2. Asada, K.; Inoue, M.; Uchida, Y.; Kameno, S.; Fujisawa, K.; Iguchi, S.; Mutoh, M. A Helical Magnetic Field in the Jet of 3C 273. *Publ. Astron. Soc. Jpn.* **2002**, *54*, L39–L43.
3. Hovatta, T.; Lister, M.L.; Aller, M.F.; Aller, H.D.; Homan, D.C.; Kovalev, Y.Y.; Pushkarev, A.B.; Savolainen, T. MOJAVE: Monitoring of Jets in Active Galactic Nuclei with VLBA Experiments. VIII. Faraday Rotation in Parsec-scale AGN Jets. *Astron. J.* **2012**, *144*, 105.
4. Mahmud, M.; Coughlan, C.P.; Murphy, E.; Gabuzda, D.C.; Hallahan, D.R. Connecting magnetic towers with Faraday rotation gradients in active galactic nuclei jets. *Mon. Not. R. Astron. Soc.* **2013**, *431*, 695–709.
5. Gabuzda, D.C.; Cantwell, T.M.; Cawthorne, T.V. Magnetic field structure of the extended 3C 380 jet. *Mon. Not. R. Astron. Soc.* **2014**, *438*, L1–L5.
6. Gabuzda, D.C.; Reichstein, A.R.; O'Neill, E.L. Are spine-sheath polarization structures in the jets of active galactic nuclei associated with helical magnetic fields? *Mon. Not. R. Astron. Soc.* **2014**, *444*, 172–184.
7. Gabuzda, D.C.; Knuettel, S.; Reardon, B. Transverse Faraday-rotation gradients across the jets of 15 active galactic nuclei. *Mon. Not. R. Astron. Soc.* **2015**, *450*, 2441–2450.
8. Gabuzda, D.C.; Knuettel, S.; Bonafede, A. Evidence for a toroidal magnetic-field component in 5C 4.114 on kiloparsec scales. *Astron. Astrophys.* **2015**, *583*, A96.
9. Abraham, Z. Precession, beaming and the periodic light curve of OJ287. *Astron. Astrophys.* **2000**, *355*, 915–921.
10. Caproni, A.; Abraham, Z. Precession in the Inner Jet of 3C 345. *Astrophys. J.* **2004**, *602*, 625–634.
11. Beaklini, P.P.; Abraham, Z.; Dominici, T.P. Detection of an Increase in the Flux Density at 43 GHz from Blazar PKS 1510-089 Since August, 2011. Available online: http://www.astronomerstelegram.org/?read=3799 (accessed on 20 August 2016)
12. Caproni, A.; Abraham, Z.; Monteiro, H. Parsec-scale jet precession in BL Lacertae (2200+420). *Mon. Not. R. Astron. Soc.* **2013**, *428*, 280–290.
13. Lister, M.L.; Aller, M.F.; Aller, H.D.; Homan, D.C.; Kellermann, K.I.; Kovalev, Y.Y.; Pushkarev, A.B.; Richards, J.L.; Ros, E.; Savolainen, T. MOJAVE XIII. Parsec-Scale AGN Jet Kinematics Analysis Based on 19 years of VLBA Observations at 15 GHz. *Astron. J.* **2016**, *152*, 12.
14. Coughlan, C.; Murphy, R.; Mc Enery, K.; Patrick, H.; Hallahan, R.; Gabuzda, D. First results from 18-22cm VLBA polarisation observations of the MOJAVE-I AGNs. *ArXiv E-print* **2011**, arXiv:astro-ph.CO/1101.5942.
15. Rusk, R.E. Brightness and Polarization Structure of Compact Radio Sources. Ph.D. Thesis, University of Toronto, Toronto, ON, Canada, 1988.
16. Taylor, A.R.; Stil, J.M.; Sunstrum, C. A Rotation Measure Image of the Sky. *Astrophys. J.* **2009**, *702*, 1230–1236.
17. Murphy, E.; Gabuzda, D. Monte Carlo Studies of Transverse Faraday Rotation Profiles. *Eur. Phys. J. Web Conf.* **2013**, *61*, 07005.
18. Contopoulos, I.; Christodoulou, D.M.; Kazanas, D.; Gabuzda, D.C. The Invariant Twist of Magnetic Fields in the Relativistic Jets of Active Galactic Nuclei. *Astrophys. J. Lett.* **2009**, *702*, L148–L152.
19. Christodoulou, D.M.; Gabuzda, D.C.; Knuettel, S.; Contopoulos, I.; Kazanas, D.; Coughlan, C.P. Dominance of outflowing electric currents on decaparsec to kiloparsec scales in extragalactic jets. *Astron. Astrophys.* **2016**, *591*, A61.